Author's Accepted Manuscript

www.elsevier.com/locate/talanta

Design of a redox-active surface for ultrasensitive redox capacitive aptasensing of aflatoxin M1 in milk

Sondes Ben Aissa, Abdelmoneim Mars, Gaelle Catanante, Jean-Louis Marty, Noureddine Raouafi

PII: S0039-9140(18)31177-9
DOI: https://doi.org/10.1016/j.talanta.2018.11.026
Reference: TAL19259

To appear in: *Talanta*

Received date: 10 August 2018
Revised date: 5 November 2018
Accepted date: 8 November 2018

Cite this article as: Sondes Ben Aissa, Abdelmoneim Mars, Gaelle Catanante, Jean-Louis Marty and Noureddine Raouafi, Design of a redox-active surface for ultrasensitive redox capacitive aptasensing of aflatoxin M1 in milk, *Talanta,* https://doi.org/10.1016/j.talanta.2018.11.026

Design of a redox-active surface for ultrasensitive redox capacitive aptasensing of aflatoxin M1 in milk

Sondes Ben Aissa[a,b], Abdelmoneim Mars[a], Gaelle Catanante[b], Jean-Louis Marty[b,*], Noureddine Raouafi [a,*]

[a]Université de Tunis El Manar, Faculté des Sciences de Tunis, Laboratoire de Chimie Analytique et Electrochimie (LR99ES15), Sensors and Biosensors Group, Campus Universitaire de Tunis El Manar, 2092, Tunis, Tunisia.

[b]Laboratoire BAE, Université de Perpignan Via Domitia, 52 Avenue Paul Alduy, 66860 Perpignan cedex 9, France.

jlmarty@univ-perp.fr

noureddine.raouafi@fst.utm.tn

[*]Corresponding authors: Tel. :+216 55 985 599

[*]Corresponding authors: Tel.:+216 55 985 599

Abstract:

Herein, we report the design of a novel label-free aptasensor based on ferrocene and silicon nanoparticles (SiNPs) for ultrasensitive detection of aflatoxin M1 (AFM1) in milk. Given that silicon nanomaterials stand out by their high capacitive power, we used them to develop a novel capacitive transduction system based on electrochemical capacitance spectroscopy (ECS). This strategy relies on the changes of the redox capacitance signal owed to the surface-tethered ferrocene film, by performing electrochemical impedance spectroscopy (EIS) measurements without using an external redox probe. The redox capacitance variation was found to correlate well with the increasing concentrations of AFM1 in the linear range from 10 to 500 fmol*L-1 with a sensitivity of 0.46 μF*fM-1*cm -2. Furthermore, the aptasensor allowed to reach very low limits of detection and quantification equal to 4.53 fM and 14.95 fM, respectively. The platform revealed a high selectivity toward the target analyte, and it was applied to quantify very low concentrations of AFM1 in commercial pasteurized milk. Finally, the results of real sample analysis were successfully gauged against those obtained using commercially available enzyme-linked immunoassay (ELISA) kits.

Keywords:
Capacitive detection; Aflatoxin M1; DNA-Aptamer; silicon nanoparticles; Ferrocene; Biosensor.

1. Introduction

Aflatoxins (AFs), which are mainly produced by *Aspergillus Flavus* and *Parasiticus*, growing on plants and foodstuffs stored under inappropriate conditions, represent the most studied group of mycotoxins [1]. Among AFs, aflatoxin B1 (AFB1) is the most recurrent and toxic food/feed contaminant. However, subsequent exposure of contaminated feed to lactating mammals metabolizes AFB1 to aflatoxin M1 (AFM1) by hydroxylation mechanism. Unfortunately, this 4-hydroxymetabolite, present in milk and derivatives, remains toxic and represents serious health hazards for human and animals even after pasteurization and dairy products processing [2]. In 2002, International Agency for Research on Cancer (IARC), has changed the classification of this aflatoxin from Group 2B (possibly carcinogenic to humans) to Group 1 (carcinogenic to human) [1], after confirmation of its serious oxidative damages due to intracellular radical generation, DNA intercalation, base impairment, birth defects, and genetic mutation [3-4]. Subsequently, the maximum admissible levels of AFM1 have been set at 50 $ng \cdot kg^{-1}$ and 25 $ng \cdot kg^{-1}$ for adults and infants, respectively, according to European standards [5].

One of the effective ways to limit AFM1 contamination is timely detection. However, conventional detection methods are usually costly, time-consuming and require skilled personnel to be operated. AFM1 sensing in milk has been previously carried out using several methods such as liquid chromatography/MS [6], HPLC coupled to fluorescence detector [7], surface plasmon resonance [8], surface plasmon-enhanced fluorescence spectroscopy [9] and ELISA [10-11]. Alternatively, the field of biosensors for food safety and detection of contaminants, especially levels of AFM1 in milk, is growing quickly. Within, electrochemical aptamer-based biosensors have received considerable attention, thanks to several inherent advantages such as their good sensitivity, amenability, cost-effectiveness and rapidity of response, which enable direct analysis in real-time.

So far, several researches focusing on the electrochemical aptasensing of AFM1 have reported the use of a 21-mer DNA aptamer, which showed a great affinity to the targeted mycotoxin through the formation of a stable antiparallel G-quadruplex [2]. Recently, Nguyen *et al.* [12] elaborated a label-free AFM1 aptasensor based on Fe_3O_4/polyaniline composite. The composite film serves as a scaffold to immobilize amine-terminated anti-AFM1 aptamer using glutaraldehyde as a crosslinker. Cyclic and square wave voltammetries revealed a good sensitivity in the range of 6-60 $ng \cdot L^{-1}$ with a detection limit of 1.98 $ng \cdot L^{-1}$. Further, Istamboulié and co-workers [13] have developed an impedimetric aptasensor based on screen-

printed carbon electrodes (SPCEs) for AFM1 determination in milk using the same 21-mer DNA aptamer. This work involves the covalent immobilization of aptamer on the carboxylbenzene modified-SPCE through carbodiimide chemistry. Aptamer-AFM1 interaction induced an increase in charge-transfer resistance, allowing AFM1 detection in the range from 2 to 150 $ng \cdot L^{-1}$ (LoD = 1.15 $ng \cdot L^{-1}$). Another aptasensor was designed by Dinçkaya *et al.* [14] using the interaction between thiol-modified aptamer with gold nanoparticles *via* self-assembled monolayer approach. The impedimetric biosensor provided a linear response to aflatoxin M1 over the concentration range of 1–14 $ng \cdot mL^{-1}$ and it was applied to detect the mycotoxin in milk samples.

The effectiveness of electrochemical detection depends not only on reliable bio-recognition elements such as aptamers, but also on a sensitive transduction method. Consequently, efforts have been recently devoted to searching for new transduction approaches that can optimize the applicability of conventional electrochemical techniques, particularly electrochemical impedance spectroscopy (EIS), in order to enhance the signal sensitivity and reach low detection limits. In this context, Bueno and Davis research groups recently proposed the impedance-derived capacitance or electrochemical capacitance spectroscopy (ECS) approach as a better alternative [15-19]. And so, they have largely exploited the ECS methodology in biosensing, mostly on gold electrodes for the detection of protein biomarkers, using antibodies as bioreceptors. Basically, ECS measures the interfacial capacitance of the electrode which is the nanoscale equivalent of the chemical capacitance when the electrode is embedded into an electrolyte, such as in the EIS measurements [20]. In a non-faradic system or faradic with redox probe in solution, this electrochemical capacitance would be governed by the inherent ionic double layer capacitance (C_{dl}). However, when the redox probe is confined to the electrode surface, a new pseudo-capacitance called "redox capacitance (C_r)" is observed, which depends on the density-of-states of the confined redox probe. Interestingly, performing EIS measurements at the half-wave potential of this confined redox system (redox-in potential) maximizes the contribution of C_r on shifting the total capacitance, while the C_{dl} value (monitored at the redox-out potential) would be almost constant and its contribution can be therefore neglected. [21].

Experimentally, C_r corresponds to the diameter of the semicircle obtained in Nyquist capacitive plots. The latter signals are converted from the well-known Nyquist EIS plots. Briefly, complex capacitance $C^*(\omega)$ can be calculated by mathematical conversion of the impedance complex function $Z^*(\omega)$ using the relationship $C^*(\omega) = 1/j\omega Z^*(\omega)$, where ω is the angular frequency and j the imaginary number [18]. According to Bueno *et al.* [19], the redox

capacitance of a faradaic probe (such as ferrocene) confined within a molecular film, is a sensitive function of the analyte concentration when that film is additionally capable of selectively recognizing a target from the solution. This suggests that EIS-derived complex capacitance signal can be used to generate an interfacial charging signal that arises solely from the redox activity of a redox-active-tethered group and depends very sensitively of its electrostatic environment [19]. This technique has been proved interesting for biosensing allowing measurements in buffered solutions without the need to add an external faradic probe, nor theoretical modeling by an equivalent circuit such as in electrochemical impedance spectroscopy [20].

On the other hand, nanobiosensors have shown a potential growth with the revolutionary advancement in nanomaterials synthesis field. Recently, several nanostructured materials have been exploited to enhance biosensing signal depending on the adopted transduction system [22]. In our case, aiming to amplify capacitive signal, we proposed to integrate semi-conductive nanomaterials, particularly silicon nanoparticles, known for their high capacitive power [23-24].

In this paper, we report the use of ferrocene-modified silicon nanoparticles deposited on a polymer-functionalized SPCE as a transducing platform. After that, anti-AFM1 aptamer was covalently immobilized on this surface to achieve design of the aptasensor. The resulting capacitive platform is able to detect AFM1 in doped buffer solutions and to successfully quantify it in milk samples. In order to validate the aptasensor response, the latter was gauged against the results obtained using a commercial immunoassay kit. It is worth mentioning that the electrochemical aptasensors reported so far for the detection of mycotoxins are based either on potentiometric, amperometric or impedimetric transduction techniques. To the best of our knowledge, we demonstrate for the first time the feasibility of electrochemical capacitance spectroscopy to detect mycotoxins using low-cost disposable SPCEs.

2. Experimental section

2.1. Chemicals and materials

All the chemicals; sodium phosphate dibasic, potassium phosphate monobasic, magnesium chloride, potassium chloride, sulfuric acid (98%), sodium chloride, ethanol (98%), hydrochloric acid, N-hydroxysuccinimide (NHS), N-(3-dimethylaminopropyl)-N′-ethylcarbodiimide hydrochloride (EDC), (3-Aminopropyl) triethoxysilane (APTES), ascorbic acid, ferrocene dicarboxylic acid (>98%), aluminum chloride, silica gel 60 mesh and fluorescent silica-coated aluminum TLC plates were obtained from Sigma-Aldrich (Germany) and used without further purification.

AFM1 (MW = 328.28 g.mol^{-1}) produced by *Aspergillus flavus*, OTB produced by *Aspergillus ochraceus* and picrotoxin (97%) were purchased from Sigma-Aldrich (Germany). AFM1-aptamer of 21-mer sequence 5'-ACT GCT AGA GAT TTT CCA CAT-3', described in [12], was purchased from Biomers (Germany) bearing a terminal amine at the 5' end.

2.2. Apparatuses

All impedance and cyclic voltammetry measurements were performed in PBS solutions (pH 7.4) using a PC-controlled Metrohm Autolab PGSTAT M204 (Utrecht, Netherlands). The electrochemical workstation was controlled with NOVA software (v2.0) to collect and analyze data. Screen printed carbon electrodes from Orion High-Tech (Spain) were used with a conventional three-electrode configuration (Fig S.1 in supplementary data). Scanning electron microscope (SEM) images were obtained using a field-emission SEM (Merlin, CarlZeiss). A thermostatic centrifuge ScanSpeed 1730R (LoboGene A/S, Denmark) was used to pretreat milk samples. All the solutions were prepared in deionized water (>18.2 MΩ.cm) produced using Milli-Q system.I'screen AFLA M1 ELISA kit (MA440) for aflatoxin M1 quantitative analysis in milk was purchased from Tecna (Italy), and optical density readings were performed using Multiskan EX 100-240V microplate photometer, from Thermo Fisher scientific.

2.3. Design of the aptasensor

We developed a new aptasensor using stepwise modification of carbon screen printed working electrodes. In a first step, the carbon surface was functionalized with Poly(p-phenylenediamine)/ silicon nanoparticles nanocomposite to amplify the background

capacitive signal. Then, the ferrocene diacid was covalently bound to the amine-terminated ligands *via* carbodiimide crosslinking chemistry. Finally, the second free carboxylic group was used to immobilize the anti-AFM1 aptamer *via* amide chemistry. The different steps are schematically presented in figure 1.

2.3.1. *Poly(p-phenylenediamine) synthesis*

Poly(p-phenylenediamine) (PpPD) was synthesized by in situ chemical oxidative polymerization according to Lei *et al.* [25]. Cyclic voltammetry of PpPD product showed a reversible faradic peak, which remains stable after 25 successive scans. The capacitive current has increased too. Moreover, the polymer immobilization on working electrode was achieved by drop-casting. The voltammetric cycling different scan rates from 50 to 500 $mV.s^{-1}$ revealed a linear relationship between PpPD oxidative peak current and the scan rate, thus confirming an adsorption-controlled electrochemical process (*cf.* Fig. 2).

2.3.2. *Synthesis of silicon nanoparticles*

A recently published quick one-step method to synthetize water-dispersible silicon nanoparticles (SiNPs) according by Chen *et al.* [24] was adopted to prepare the nanomaterial (*cf*. Fig. 3 below).

So far, silicon nanoparticles are widely reported for fluorescence assays. However, to the best of our knowledge their electrochemical applications have not been investigated yet. Electrochemical characterization of the obtained SiNPs solution was performed using CV and ECS techniques.

Obtained results highlight a high capacitive power due to semi-conductive properties of this nanomaterial (*cf*. Fig. 4).

The size of the prepared silicon nanoparticles was estimated using transmission electron microscopy (TEM) to find aggregates of nanoparticles of approximately 50 nm. This aggregation is probably due to abundant amine ligands. (*cf.* Fig S.2)

2.3.3. *Stepwise fabrication strategy*

Prior to modification, SPCE surface was electrochemically activated and cleansed by scanning the potential for 15 consecutive scans from -1.5 to +1.5 V vs. Ag/AgCl at 100 $mV.s^{-1}$ in a solution of 0.5 M sulfuric acid diluted in 0.1M KCl. Once cleaned, the SPCE was thoroughly washed with deionized water, and then working electrode was used as substrate for step-by-step build-up procedure. Firstly, 5 µL of PpPD suspension were dropped was allowed to dry at room temperature (RT) for 15 min. Secondly, 5 µL of SiNPs solution were added on PpPD-modified SPCE to ensure its physical adsorption *via* hydrogen bonds and dried at RT. After that, the surface was functionalized with 5mM ferrocene dicarboxylic acid, previously activated using EDC (100 mM) and NHS (25 mM) mixture, to undergo covalent coupling. In the last step, an optimized concentration of 1µM anti-AFM1 aptamer was added to the already activated ferrocene carboxylic acid groups to form covalent amid bonds with the terminal amine from the aptamers. After 60 min of incubation, the excess of the aptamer was washed off with buffer solution and the aptamer was kept at 4 °C until use.

2.4. Electrochemical measurement and sensing of aflatoxin M1

2.4.1. *Electrochemical measurements*

Since working in non-faradic regime is mandatory to obtain exploitable ECS response [18], PBS solution containing 2 mM $MgCl_2$ was used as supporting electrolyte. Cyclic voltammetry measurements were performed by scanning the potential from -0.5 to +0.8 V *vs.* Ag/AgCl at a scan rate of 100 $mV.s^{-1}$. Electrochemical impedance spectroscopy experiments were carried out at an applied potential of +0.1V (*vs.* Ag/AgCl), obtained from the equilibrium redox potential of immobilized ferrocene with a frequency range from 100 kHz to 0.1 Hz, an AC amplitude of 10 mV and a sampling rate of 50 points.

The impedance spectra were directly converted to their corresponding capacitive spectra using NOVA v2.0 software and plotted as complex plane diagrams (Nyquist plots; imaginary capacitance C" vs. real capacitance C'). Subsequently, redox capacitance "C_r" values were extracted graphically by fitting the obtained semi-circles. More precisely, the complex $Z^*(\omega)$ impedance function was converted into $C^*(\omega)$ capacitance function through the physical

definition $Z^*(\omega) = 1/j\omega C^*(\omega)$ in which ω is the angular frequency. Real and imaginary capacitance components were obtained respectively from reported equations $C'' = \varphi Z'$ and $C' = \varphi Z''$ where $\varphi = (\omega|Z|^2)-1$ and $|Z|$ is the modulus of Z^*[19].

2.4.2. *Sensing of the AFM1*

The aptasensor anti-AFM1/Fc/SiNPs-PpPD/SPCE was incubated, under optimized conditions, for 30 min at 45 °C with different concentrations of AFM1 solutions. Then, electrodes were thoroughly washed 3 times with the buffer solution, to immediately record their capacitive response. All electrochemical measurements were carried out in three repetitions by dropping 50 µL of buffer solution onto SPCE working area.

2.4.3. *Detection of AFM1 level in milk*

2.4.3.1. AFM1 aptasensing

In order to evaluate the applicability of AFM1 aptasensor in real matrix, we tested the developed platform to detect AFM1 in commercial pasteurized milk samples using the method of standard additions. First, we spiked three milk samples (in triplicate) with 0, 10 and 45 pM of AFM1 standards by adding 10 µL of appropriate toxin solution in acetonitrile (taking into consideration dilution factor) to a sample volume of 990 µL. Spiked samples were heated in a water-bath at +40 °C for 30 min as preliminary pretreatment step. Subsequently, each milk sample was mixed with HPLC grade methanol (1/3 v/v) as a best recommended method for lipid and protein depletion. A total volume of 800µL was then centrifuged for 5 min at 6000 rpm at RT, as described by Istamboulié *et al.* [13]. After centrifugation, the fatty cream was discarded and resultant supernatant was carefully recovered without reaching the heavy precipitate (See picture in Fig S.5).

Afterward, we diluted the recovered supernatant 1000 folds with PBS buffer for a direct analysis using the developed aptasensor. We found that this dilution is mandatory because of two main reasons i) to minimize the effect of methanol on analyte/aptamer recognition process and ii) to adjust the response to the concentrations level in the established dynamic range. Finally, following similar incubation conditions as specified for standards (30 min at 45°C), we recorded the capacitive electrochemical response of raw and spiked supernatants.

2.4.3.2. ELISA detection

In a second step, the biosensor response was challenged against results obtained with a competitive enzyme immunoassay using a commercial ELISA kit. For that purpose, we have

chosen "I'screen AFLA M1 milk" (cod. MA441 - MA440), a specific kit for the quantitative analysis of aflatoxin M1 in milk matrix. The assay is performed in plastic microwells, which have been coated with anti-aflatoxin M1 antibodies. Aflatoxin M1 standard solutions and samples are added to the microwells. Following the suppliers recommendations, 3 incubation steps were performed; during the first incubation, free aflatoxin M1 molecules are bound to the anti-aflatoxin M1 antibodies. Any unbound substance is then removed in a washing step. A second incubation is performed with an aflatoxin-HRP conjugate, which covers all the remaining free binding sites of the antibody. The bound enzyme activity is determined by adding a fixed amount of a chromogenic substrate. The enzyme converts the colourless chromogen into a blue product during the third incubation. The addition of the stop reagent leads to a color change from blue to yellow. Then, absorbance is measured by a microplate reader at 450 nm. The color development is inversely proportional to the aflatoxin M1 concentration in the sample as we can see in the calibration curve illustrated in supporting data (Fig S.6).

3. Results and discussion

3.1. Design of the aptasensing platform

The stepwise modification of the electrode surface to build the aptasensing platform was monitored by cyclic voltammetry and EIS-derived capacitance spectroscopy in non-faradic regime. Additionally to typical square-shaped voltammograms, due to the high charge/discharge capacity of the electrode owed to the addition of the SiNPs, figure 5 (A) shows the voltammograms, recorded after each modification step of the SPCE, evidencing a ferrocene redox peaks located at potential of 0.1 V (half-wave potential of the ferrocene/ferrocenium couple, Fc/Fc^{+}), at which EIS measurements are performed. Ferrocene faradic signal in CV was high enough to compensate important capacitive current.

As shown in fig. 5 (B), the adsorption of PpPD polymer induced a slight increase in the double layer capacitance, against a considerable increase upon SiNPs addition. Accordingly, this fivefolds increase in capacitance (i.e. ~10 to ~50 µF), obtained after functionalization of working electrode with the nanocomposite, is mainly attributed to semi-conductive properties of silicon nanoparticles. After the immobilization of ferrocene, the amine oxidation wave

located *ca.* 0.8 V disappears because of their participation in redox inactive amide groups. Furthermore, the capacitance raised slightly because at this particular potential, ferrocene centers are positively charged creating thus adding a new "redox capacitance" contribution. Herein, the wisdom behind choosing the dicarboxylic acid ferrocene is that it will act as i) a linker between the surface and the aptamer and ii) its redox signal will probe the aptamer folding when it recognizes the AFM1.

After aptamer covalent coupling, reversible faradic peaks in CV graphs disappeared, which proves an effective immobilization. Correspondingly, ECS signal decreased slightly, which can be referred to negatively charged aptamers that induced an electronic perturbation in the vicinity of ferrocene moieties, and therefore a diminution of redox capacitance value.

Upon target recognition, the aptamer folding through a G-quadruplex structure heightens this electronic perturbation *via* redistribution of aptamer negative charges in the bio-recognition layer. Consequently, the formed aptamer-AFM1 complexes alter the density-of-states of ferrocene as a confined redox probe. This assumption can explain the obtained ON/OFF response, clearly observed in Fig.5 (B) after incubation of 100fM of AFM1. In fact, the redox-probe-confined surface contributes to a substantial potential-dependent interfacial charging that can be sensitively probed and frequency-resolved by impedance-derived capacitance spectroscopy [16]. This capacitive sensory system is based on the high sensitivity of generated charging fingerprint to redox group environment.

3.2. Analytical performances of the aptasensor

3.2.1. *Dynamic range*

Since strict AFM1 levels are allowed in commercial milk, we tried to detect very low concentrations of this mycotoxin. Using the ECS transduction, sensing range was successfully lowered to reach a good response in femtomolar scale (Fig.6A). The interaction between AFM1 and the aptamer layer induced a proportional decrease of the redox capacitance, which is in agreement with previously published works [16].

Further, to compare the results obtained from different electrodes and to obtain independent results, an analytical parameter ΔC_r, is defined using absolute redox capacitance values (in µF) as showed in the following equation:

$$\Delta C_r(\mu F) = C_r(Apt) - C_r(Apt/AFM1)$$

Where, $C_{r\ (Apt/AFM1)}$ is the redox capacitance of the aptasensor calculated after incubation with AFM1 and $C_{r(Apt)}$ is the redox capacitance of the blank aptasensor response (incubation of buffer without target). It is to note that C_r values were measured by the projection of the semicircle diameter in the axis C', corresponding to the frequency value where C" is minimized (at low frequencies) as detailed in [15].

A linear calibration plot was constructed (Fig. 6B) by using the redox capacitance variation results in the concentration range 10-500 fmol.L^{-1} (corresponding to 3.3-165 pg.L^{-1}). A good sensitivity value of 0.46 (±0.02) µF.fM^{-1}.cm^{-2} was obtained (Given a WE area of 0.125 cm^2). This sensitivity is calculated based on the slope of a linear regression fitting (OriginPro v9) having the following equation y = 0.058 (x) + 2.19 (R^2 = 0.983). Every concentration experiment was carried out in triplicate, with an average RSD of capacitance response around 5.44%.

This detection domain does not include the concentration values corresponding to the maximum AFM1 levels set in European Union for adult dairy food (50 ng·kg^{-1}) and for infant products (25 ng·kg^{-1}). Thus, milk samples have to be diluted further for AFM1 quantification in real matrix, which may be of high interest in decreasing the matrix effect.

3.2.2. *Detection limits and comparison with literature*

A limit of detection (LOD) equals to 4.53 fM (1.48 pg.L^{-1}) is calculated by using the three times "σ/s" value. In this "σ" represents the standard deviation and "s" represents the slope of the calibration curve. The limit of quantification (LOQ) is obtained by multiplying the LOD per a coefficient of 3.3 (LOQ = 3.3*LOD) to obtain a value of 14.95 fM (4.9 pg.L^{-1}). It is to highlight that this is the first work reporting such low limits for aflatoxin M1 sensing (*cf.* Table 1).

The as-prepared aptasensor shows better analytical performances in terms of detection limits compared to other reported electrochemical biosensors for AFM1 detection as summarized in table 1. Also, it is much more sensitive since it allows detecting sublevels of part-per-trillion of the target analyte. Although the detection ranges are different, one can see that almost all the sensors have two decades linear ranges.

Currently, we believe that the main reason behind sensitivity enhancement using our aptasensing system compared to other reported works (in which the same aptamer sequence was used), is simply imputable to the use of ECS as a novel transduction method, tested for the first time in the AFM1detection. More clearly, ECS signals are able to report the smallest

variations in the energetic level of the redox tethered-film. This signal variations are occurred at the half-wave potential of the system (at which EIS measurements are performed). This response is quantified through the redox capacitance term. Based on aptamer's high selectivity, this suggests that only target analyte recruitment will induce an ultrasensitive capacitive response. Contrary to conventional EIS technique (based on electron transfer resistance), which is governed by a free redox probe in bulk solution, ECS approach is able to report the nanometric fingerprint of a well-confined redox film.

Table 1: Comparison of previously reported electrochemical biosensors for AFM1 detection with current work

Electrochemical transduction technique	Detection range (ppt)	Limit of detection (ppt)	References
Chronoamperometry	30 - 160	25	[26]
CV and SWV	6 - 60	1.98	[12]
EIS	2 - 150	1.15	[13]
EIS	6.25 - 100	1	[27]
EIS and LSV	15-1000	15	[28]
Chronoamperometry	5 - 500	10	[29]
ECS	0.003 – 0.165	0.0015	This work

3.2.3. *Selectivity*

Selectivity is one of the most important features of a biosensor. It is insured by the ability of bioreceptors to detect the specific analyte in a sample containing other interfering molecules. The dissociation constant of the employed aptamer has not been reported in literature [4]. Therefore, it was mandatory to evaluate the response of the aptamer-based capacitive sensor against other mycotoxins produced by other fungi, to confirm its selectivity toward AFM1. The histogram below highlights the good specificity of aptasensor to AFM1. The presented data (*cf.* fig 7) displays the response of the biosensor, which is six folds higher with target mycotoxin comparing to signal induced by the other mycotoxins for a concentration of the target analyte or the interfering toxins equals to 1 pM.

3.3. Real sample analysis

3.3.1. *AFM1 quantification in milk*

EIS measurements were carried out in the same conditions as described for the detection of AFM1 in spiked solutions, to be then converted to ECS signals. Figure 8.A shows the obtained capacitive signals while figure 8.B plots the linear proportionality in terms of redox capacitance variation (error bars corresponds to 3 repetitions). The unspiked sample revealed a slight change of redox capacitance compared to the blank response. However, subsequent spiking with 10 and 45 pM of AFM1 standard solutions decreased more the redox capacitance signal.

As reported by Harris [30], the standard addition method allows an analytical estimation of the unknown concentration ([X]), from the slope (a) and the intercept (b) of the linear relation ([X]=b/a). Obtained results are summarized in table 2. Accordingly, the amount of AFM1 in the tested milk sample was estimated at 4.66 (±0.135) $ng.L^{-1}$, which is largely lower than tolerated levels set by European Union norms. The tested milk batch is therefore compliant without risk to human health.

Table 2 Standard additions results for the real sample analysis

AFM1 concentration (fM*) *Dilution factor F=1000	Aptasensor's response ΔCr (µF)	Standard additions equation	AFM1 amount estimation in DRS
0	1.02	y = a x + b a = 0.077 b = 1.09 R^2 = 0.99	14,21 (±0,412) fM 4,66 (±0,135) ppt RSD = 2.9%
10	1.93		
45	4.54		

3.3.2. *Test validation for the real sample*

In order to validate the response of the biosensor, the same milk samples were tested using a commercial ELISA assay. Following the supplier recommendations, a calibration curve was established between 5 and 250 $ng.L^{-1}$ and AFM1 quantities in samples were determined using a provided Excel spreadsheet (Fig S.6).

The obtained results indicated that AFM1 concentration in milk sample is equal or less than 5 $ng.L^{-1}$ (below the kit's limit of quantification of 5 ppt), which confirms the analytical reliability of results provided by our capacitive aptasensor.

4. Conclusion

We designed a novel capacitive disposable biosensor using silicon nanoparticles to amplify the double layer capacitance component and a ferrocene layer as a redox capacitance element. This aptasensor has shown high performances for the detection of aflatoxin M1 in milk samples with minimal pretreatment process. The analytical device was able to quantify very low amounts of AFM1, making it a great alternative to conventional techniques with usually restricted detection limits. To achieve a specific ECS detection, an accurate control of the biosensing interface design was established, using a ferrocene-functionalized confined layer. To the best of our knowledge, this work reports for the first time the combination of SPCEs and ECS methodology, which is advantageous in disposability, portability and ultra-high sensitivity for AFM1 detection in real samples. Furthermore, it was shown that the bioplatform was able to detect AFM1 in milk without interferences with matrix effect. This merit comes from its ability to quantify analyte in extremely diluted sample. Real milk samples were successfully analyzed and a good correlation was obtained with the data achieved using a conventional immunoassay kit. These results open up the path for designing highly-sensitive and cost effective aptasensors for other environmental or biomedical applications.

Acknowledgements

The authors are grateful for financial support from ERASMUS+ program for the mobility grant "EMIC" awarded to SBA. The authors also acknowledge the financial support for the Tunisian Ministry of Higher Education and Scientific Research for Lab LR99ES15 funding. University of Tunis El Manar is acknowledged for mobility grant "Bourse d'alternance" for SBA.

Conflicts of Interest

The authors declare no conflict of interest.

References

[1] A.M. Gurban, P. Epure, F. Oancea, M. Doni, Achievements and prospects in electrochemical-based biosensing platforms for aflatoxin M1 detection in milk and dairy products, Sensors (Switzerland). 17 (2017) 1–21. doi:10.3390/s17122951.

[2] A. Sharma, G. Catanante, A. Hayat, G. Istamboulie, I. Ben Rejeb, S. Bhand, J.L. Marty, Development of structure switching aptamer assay for detection of aflatoxin M1 in milk sample, Talanta. 158 (2016) 35–41. doi:10.1016/j.talanta.2016.05.043.

[3] S. Marchese, A.Polo, A.Ariano, S.Velotto, S.Costantini, L.Severino. Aflatoxin B1 and M1: Biological Properties and Their Involvement in Cancer Development, Toxins 10, no. 6 (2018) 214. doi:10.3390/toxins10060214.

[4] A. Sharma, K. Goud, A. Hayat, S. Bhand, J.L. Marty, Recent Advances in Electrochemical-Based Sensing Platforms for Aflatoxins Detection, Chemosensors. 2017, 5, 1-15.doi:10.3390/chemosensors5010001.

[5] Official journal of the European Communities, setting maximum levels for certain contaminants in foodstuffs (Text No1881 with EEA relevance), (2006) 5–24.

[6] C. Cavaliere, P. Foglia, E. Pastorini, R. Samperi, A. Laganà, Liquid chromatography/tandem mass spectrometric confirmatory method for determining aflatoxin M1 in cow milk: Comparison between electrospray and atmospheric pressure photoionization sources, J. Chromatogr. A. 1101 (2006) 69–78. doi:10.1016/j.chroma.2005.09.060.

[7] G. Chavarría, F. Granados-Chinchilla, M. Alfaro-Cascante, A. Molina, Detection of Aflatoxin M1 in Milk, Cheese and Sour Cream Samples from Costa Rica Using Enzyme-Assisted Extraction and HPLC, Food Addit. Contam. Part B Surveill. 8 (2015) 128–135. doi:10.1080/19393210.2015.1015176.

[8] S.J. Daly, G.J. Keating, P.P. Dillon, B.M. Manning, R. O'Kennedy, H.A. Lee, M.R.A. Morgan, Development of surface plasmon resonance-based immunoassay for aflatoxin B1, J. Agric. Food Chem. 48 (2000) 5097–5104. doi:10.1021/jf9911693.

[9] Y. Wang, J. Dostálek, W. Knoll, Long range surface plasmon-enhanced fluorescence spectroscopy for the detection of aflatoxin M1 in milk, Biosens. Bioelectron. 24 (2009) 2264–2267. doi:10.1016/j.bios.2008.10.029.

[10] D. Neagu, S. Perrino, L. Micheli, G. Palleschi, D. Moscone, Aflatoxin M1determination and stability study in milk samples using a screen-printed 96-well electrochemical microplate, Int. Dairy J. 19 (2009) 753–758. doi:10.1016/j.idairyj.2009.06.004.

[11] S.C. Pei, Y.Y. Zhang, S.A. Eremin, W.J. Lee, Detection of aflatoxin M1 in milk products from China by ELISA using monoclonal antibodies, Food Control. 20 (2009) 1080–1085. doi:10.1016/j.foodcont.2009.02.004.

[12] B.H. Nguyen, L.D. Tran, Q.P. Do, H. Le Nguyen, N.H. Tran, P.X. Nguyen, Label-free detection of aflatoxin M1 with electrochemical Fe3O4/polyaniline-based aptasensor, Mater. Sci. Eng. C. 33 (2013) 2229–2234. doi:10.1016/j.msec.2013.01.044.

[13] G. Istamboulié, N. Paniel, L. Zara, L.R. Granados, L. Barthelmebs, T. Noguer, Development of an impedimetric aptasensor for the determination of aflatoxin M1 in milk, Talanta. 146 (2016) 464–469. doi:10.1016/j.talanta.2015.09.012.

[14] E. Dinçkaya, Ö. Kinik, M.K. Sezgintürk, Ç. Altuğ, A. Akkoca, Development of an impedimetric aflatoxin M1 biosensor based on a DNA probe and gold nanoparticles, Biosens. Bioelectron. 26 (2011) 3806–3811. doi:10.1016/j.bios.2011.02.038.

[15] J. Cecchetto, F.C.B. Fernandes, R. Lopes, P.R. Bueno, The capacitive sensing of NS1 Flavivirus biomarker, Biosens. Bioelectron. 87 (2017) 949–956. doi:10.1016/j.bios.2016.08.097.

[16] J. Lehr, F.C.B. Fernandes, P.R. Bueno, J.J. Davis, Label-free capacitive diagnostics: Exploiting local redox probe state occupancy, Anal. Chem. 86 (2014) 2559–2564. doi:10.1021/ac403727h.

[17] J. Piccoli, R. Hein, A.H. El-Sagheer, T. Brown, E.M. Cilli, P.R. Bueno, J.J. Davis, Redox Capacitive Assaying of C-Reactive Protein at a Peptide Supported Aptamer Interface, Anal. Chem. 90 (2018) 3005–3008. doi:10.1021/acs.analchem.7b05374.

[18] A. Santos, J.J. Davis, P.R. Bueno, Fundamentals and Applications of Impedimetric and Redox Capacitive Biosensors, J. Anal. Bioanal. Tech. S7 (2014). doi:10.4172/2155-9872.S7-016.

[19] F.C.B. Fernandes, M.S. Góes, J.J. Davis, P.R. Bueno, Label free redox capacitive biosensing, Biosens. Bioelectron. 50 (2013) 437–440. doi:10.1016/j.bios.2013.06.043.

[20] B.L. Garrote, The potentiality and limitations of electrochemical impedance spectroscopic methods for molecular film applications, University of São Paulo, 2018.

[21] J. Lehr, J.R. Weeks, A. Santos, G.T. Feliciano, M.I.G. Nicholson, J.J. Davis, P.R. Bueno, Mapping the ionic fingerprints of molecular monolayers, Phys. Chem. Chem. Phys. 19 (2017) 15098-15109. doi:10.1039/C7CP01500C.

[22] B.D. Malhotra, M.A. Ali. Chapter 1 - Nanomaterials in Biosensors: Fundamentals and Applications. Nanomaterials for Biosensors, 1–74. Micro and Nano Technologies. William Andrew Publishing. (2018) 1-74. doi:10.1016/B978-0-323-44923-6.00001-7.

[23] W.B. Adrian, Electrochemistry of Semiconductors, Current Separations, 17:3 d,1998, 87–91.

[24] S.D. Ma, Y.L. Chen, J. Feng, J.J. Liu, X.W. Zuo, X.G. Chen, One-Step Synthesis of Water-Dispersible and Biocompatible Silicon Nanoparticles for Selective Heparin Sensing and Cell Imaging, Anal. Chem. 88 (2016) 10474–10481. doi:10.1021/acs.analchem.6b02448.

[25] H. Peng, G. Ma, K. Sun, J. Mu, Z. Zhang, Z. Lei, Facile Synthesis of Poly(p -phenylenediamine)-Derived Three-Dimensional Porous Nitrogen-Doped Carbon Networks for High Performance Supercapacitors, J. Phys. Chem. C. 118 (2014) 29507–29516. doi:10.1021/jp508684t.

[26] L. Micheli, R. Grecco, M. Badea, D. Moscone, G. Palleschi, An electrochemical immunosensor for aflatoxin M1 determination in milk using screen-printed electrodes, Biosens. Bioelectron. 21 (2005) 588–596. doi:10.1016/j.bios.2004.12.017.

[27] G. Bacher, S. Pal, L. Kanungo, S. Bhand, A label-free silver wire based impedimetric immunosensor for detection of aflatoxin M1 in milk, Sensors Actuators, B Chem. 168 (2012) 223–230. doi:10.1016/j.snb.2012.04.012.

[28] A. Vig, A. Radoi, X. Muñoz-Berbel, G. Gyemant, J.L. Marty, Impedimetric aflatoxin M1immunosensor based on colloidal gold and silver electrodeposition, Sensors Actuators, B Chem. 138 (2009) 214–220. doi:10.1016/j.snb.2008.12.033.

[29] N. Paniel, A. Radoi, J.-L. Marty, Development of an Electrochemical Biosensor for the Detection of Aflatoxin M1 in Milk, Sensors. 10 (2010) 9439–9448. doi:10.3390/s101009439.

[30] D.C. Harris, Quantitative Chemical Analysis. 7th ed, W. H. Freeman, (2007) 0-7167-7041-5.

Figure 1: Schematic representation of aptasensor's development steps for AFM1 detection.

Figure 2: (A) Poly(p-phenylenediamine) synthesis route, (B) Cyclic voltammetry of PpPD product showing stability after 25 successive scans at 100 $mV.s^{-1}$, (C) PpPD oxidative peak current Vs scan rate from 50 to 500 $mV.s^{-1}$.

Figure 3: Schematic Synthesis reaction of silicon nanoparticles (SiNPs) according to Chen et al. method.

Figure 4: Electrochemical characterization of the SiNPs- modified SPCE : (a) CV graphs at a scan rate of 100 $mV.s^{-1}$ (b) Nyquist capacitive plots converted from EIS data (displayed inset) performed at an applied potential of 0.1V.

Figure 5: (A) Cyclic voltammograms performed in 0.1M PBS pH 7.4 at 100 $mV.s^{-1}$ and (B) Capacitive Nyquist plots obtained from EIS data recorded at an applied potential of 0.1V, of the different modification steps.

Figure 6: (A) Recorded Nyquist capacitive signals performed in 0.1M buffer solution after incubation in different AFM1 solutions with gradually increasing concentrations ranging from 10 to 500 fM (C'' is the imaginary and C' is the real part of capacitance). (B) Analytical plot obtained for AFM1 detection in buffer showing a linear response (R^2=0,983) wherein the RSD showed for each concentration (error bars) represents three repetitions of the same functionalized electrode.

Figure 7: Histogram showing the aptasensor's response after incubation in other mycotoxin solutions evidencing platform's selectivity toward target AFM1.

Figure 8: Real sample analysis (A) Nyquist capacitive signals of spiked milk samples (B) Obtained linear regression for standard additions calculations.

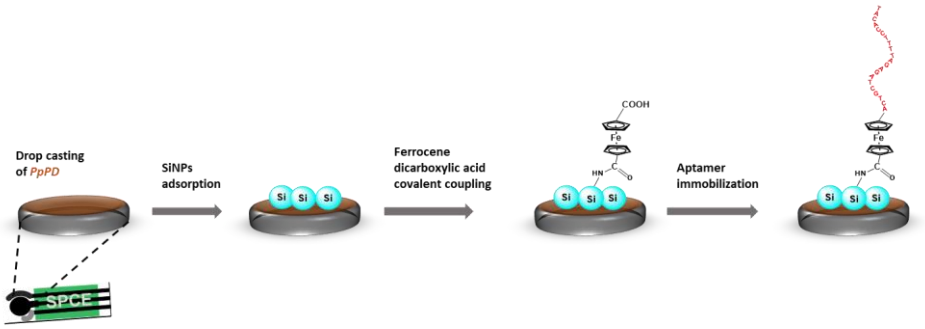

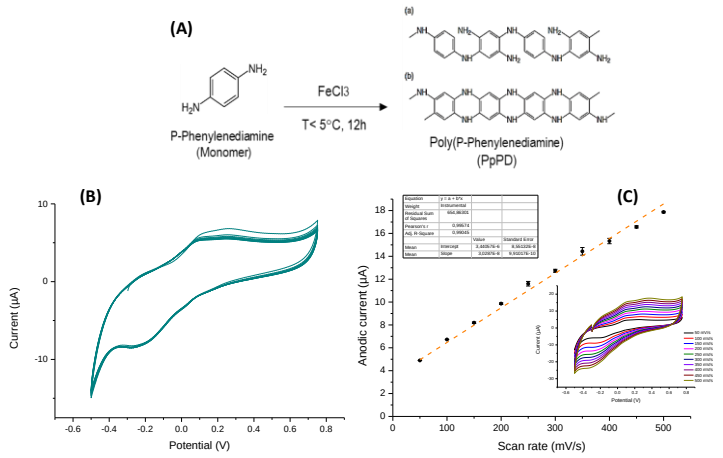

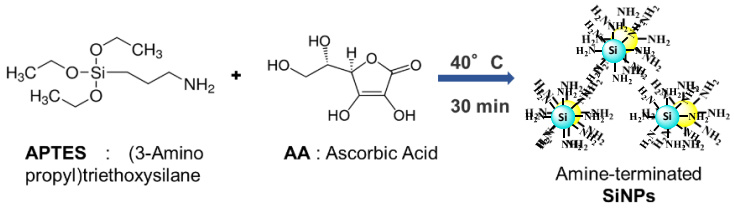

APTES : (3-Amino propyl)triethoxysilane

AA : Ascorbic Acid

Amine-terminated **SiNPs**

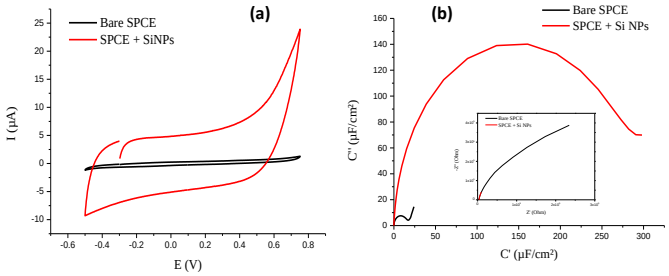

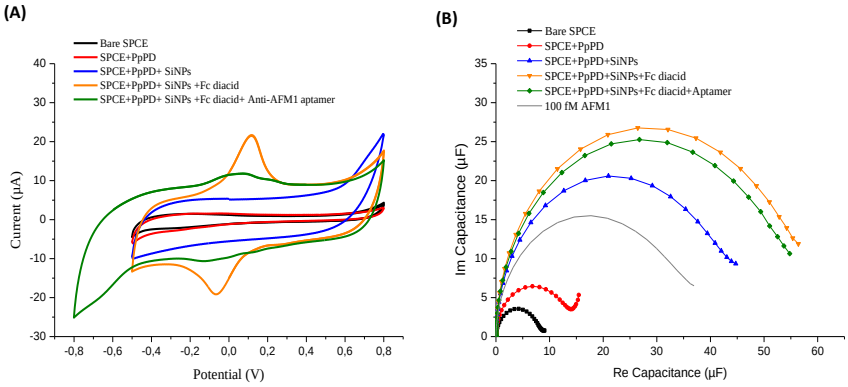

(A)

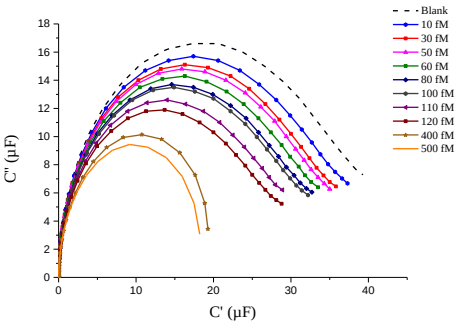

(B)

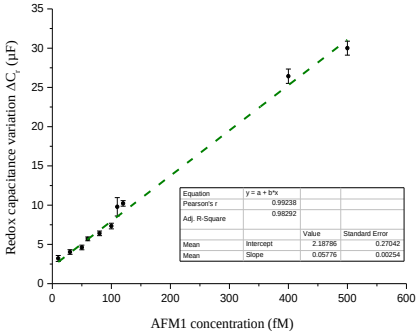

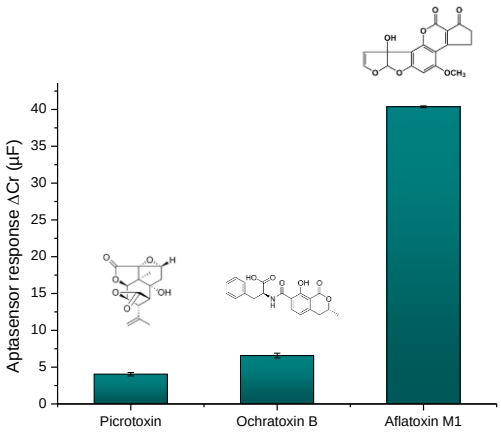

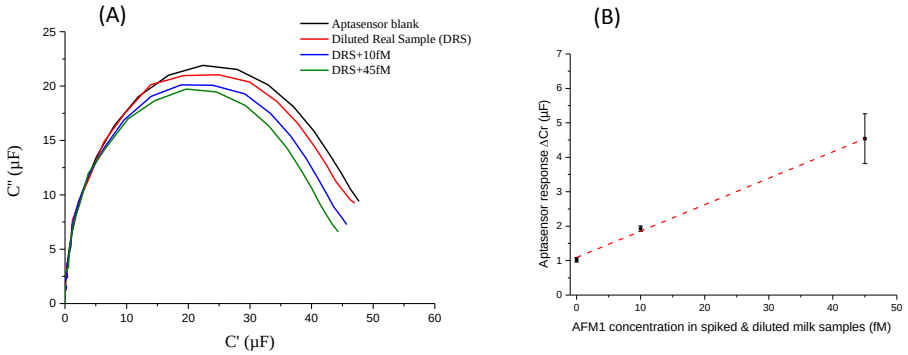

Highlights

- Development of a highly sensitive disposable aptasensor for aflatoxin M1 detection in milk using a novel electrochemical capacitance spectroscopy approach.
- The strategy relies on the changes of the redox capacitance signal owed to the surface-tethered redox film, by performing electrochemical impedance spectroscopy measurements without using an external redox probe.
- The first feasibility study of the redox capacitance transduction (ECS) using screen-printed carbon electrodes (SPCE), using modifications with ferrocene-functionalized silicon nanoparticles.
- Detection of very low amounts of target (femtomolar range) which resulted in quantifying very low concentrations of AFM1 in commercial pasteurized milk.